High-Precision Bootstrap of Multimatrix Quantum Mechanics

Henry W. Lin[1,2,*] and Zechuan Zheng[3,4,†]
[1]Leinweber Institute for Theoretical Physics, Stanford University, Stanford, California 94305, USA
[2]Jadwin Hall, Princeton University, Princeton, New Jersey 08540, USA
[3]Perimeter Institute for Theoretical Physics, Waterloo, Ontario N2L 2Y5, Canada
[4]Laboratoire de Physique de l'Ecole Normale Supérieure, ENS, Université PSL, CNRS, Sorbonne Université, Université Paris Cité, F-75005 Paris, France

(Received 15 December 2025; revised 22 February 2026; accepted 31 March 2026; published 7 May 2026)

We consider matrix quantum mechanics with multiple bosonic matrices, including those obtained from dimensional reduction of Yang-Mills theories. Using the matrix bootstrap, we study simple observables like $\langle \mathrm{tr}\, X^2 \rangle$ in the confining phase of the theory in the infinite N limit. Exploiting the symmetries of these models and applying nonlinear relaxation, we impose constraints that include traces of words of length up to 14. Our results yield rigorous bounds on the large-N ground-state dynamics, along with estimates of selected low-order observables to eight significant digits.

DOI: 10.1103/cyq8-4sd7

Introduction—Solving large N gauge theories has been a long-held dream of modern physics. An important tool in this pursuit has been Euclidean Monte Carlo lattice computations. However, this approach requires extrapolation to large N where computation becomes increasingly expensive, although physics simplifies in this limit. Another nonperturbative approach that has been comparatively less developed is the matrix bootstrap [1–4] which works directly in the infinite N, 't Hooft limit by imposing large N factorization [5].

In this Letter, we continue developing this approach by performing a high-precision bootstrap of large N bosonic matrix quantum mechanics. These include models arising from dimensional reduction of Yang-Mills (YM) theories in $D+1$ dimensions. Such $0+1$-dimensional models share some qualitative aspects with their higher-dimensional counterparts in compact spaces [7], with a similar phase diagram. More precisely, it is believed that, at large N, these quantum mechanical theories exhibit two continuous phase transitions. For low temperatures $T < T_{c,1}$, the theory is in a confining phase characterized by a $\sim O(N^0)$ free energy. At the first critical temperature, $T_{c,1}$, the theory undergoes a second-order Hagedorn transition to a deconfined phase, where the free energy scales as $O(N^2)$. Another third-order Gross-Witten-Wadia transition [8,9] occurs at a temperature $T_{c,2} > T_{c,1}$. Both transitions occur at temperatures of order one in units of the 't Hooft coupling [10–12].

A key improvement over previous bootstrap studies is the use of nonlinear relaxation techniques to deal with the nonlinear system of equations that arise after imposing a large N factorization [4]. So far, this method has been implemented in the path integral context [4,13]; in this Letter, we implement it in the Hamiltonian formalism. We also apply the ground state positivity condition (6), which dramatically boosts the precision of the bootstrap. Finally, we systematically leverage the $\mathrm{O}(D)$ symmetry of these models which was crucial in allowing us to go up to level 14.

This Letter may also be viewed as a natural continuation of [14]. The bosonic models considered here are somewhat simpler to bootstrap than the supersymmetric Banks–Fischler–Shenker–Susskind (BFSS) model studied in [14], mainly because the group-theoretic structure is less intricate. The computational methods developed in this Letter should inform future efforts, including our planned high-precision bootstrap analysis of the BFSS matrix quantum mechanics [15].

Our motivation to push the precision frontier is not merely precision for the sake of precision. In the supersymmetric BFSS case, a high-precision measurement of the thermodynamics and/or correlation functions would allow one to "experimentally" measure higher derivative corrections to Type IIa supergravity [16–25]. These corrections are currently unknown using world sheet methods. So, the high-precision bootstrap could teach us about quantum gravity. In a similar spirit, lattice Monte Carlo studies for large N Yang-Mills theory (see Ref. [26] for a review and, e.g., [27,28] for recent progress) can teach us about the effective string. We view our Letter as a starting point for a

*Contact author: hwlin@princeton.edu
†Contact author: zechuan.zheng.phy@gmail.com

Published by the American Physical Society under the terms of the Creative Commons Attribution 4.0 International license. Further distribution of this work must maintain attribution to the author(s) and the published article's title, journal citation, and DOI. Funded by SCOAP³.

bootstrap study for higher-dimensional Yang-Mills theory in the Hamiltonian [29] lattice gauge theory formalism [30].

Several appendices and Supplemental Material [33] complement this Letter. In the Appendices, we provide details on the numerical implementation, the relaxation procedure, some results on large D expansion, and further discussion of the adjoint gap. In Supplemental Material [33], we include a pedagogical example that illustrates our bootstrap framework in a simplified setting. We also describe a specific method for performing the irreducible decomposition of operators and summarize the technical steps involved in the large-D analysis.

Bootstrap ingredients—

The models: We consider systems that consist of D bosonic matrices, satisfying the commutation relations $[(X_I)_{ij}, (P_J)_{kl}] = \mathrm{i}\delta_{il}\delta_{jk}\delta_{IJ}$. Here I, J run from 1 to D. These matrices are traceless and Hermitian and transform in the adjoint of SU(N). The Hamiltonian is

$$H = \frac{1}{2}\sum_{I=1}^{D} \mathrm{Tr} P_I P_I + M^2 \mathrm{Tr} X_I X_I - \frac{g_{\mathrm{YM}}^2}{4}\sum_{I,J}^{D} \mathrm{Tr}[X_I, X_J]^2 \quad (1)$$

The ground state of this model is gauge invariant $C|\Omega\rangle = 0$, where the SU(N) gauge generators are $C = \sum_{I=1}^{D}(-\mathrm{i}[X_I, P_I] - N\mathbf{1})$. The model possesses an O(D) global symmetry, under which the fields X_I and P_I transform in the fundamental representation. The case with $M^2 = 0$ is of particular interest, as it arises from the dimensional reduction of pure Yang–Mills theory in $D+1$ dimensions. (For certain values of D, the massless theory may also be obtained by reducing supersymmetric Yang–Mills theories on tori T^d with antiperiodic boundary conditions for the fermions; see, for example, [10]).

For the massless model, we may set $g_{\mathrm{YM}}^2 = 1$ without loss of generality by performing a canonical transformation together with a rescaling of the Hamiltonian. For the massive model, the dynamics are governed by the dimensionless effective coupling $\lambda_{\mathrm{eff}} = g_{\mathrm{YM}}^2 N/M^3$.

For the $D = 2$ version, it is convenient to view SO(2) as U(1) and work with complex operators

$$Z = \frac{1}{\sqrt{2}}(X_1 + \mathrm{i}X_2), \qquad \bar{Z} = \frac{1}{\sqrt{2}}(X_1 - \mathrm{i}X_2), \quad (2)$$

and similarly $P = (1/\sqrt{2})(P_1 + \mathrm{i}P_2)$, $\bar{P} = (1/\sqrt{2}) \times (P_1 - \mathrm{i}P_2)$. Then the U(1) charge of an operator is simply the difference between (number of Z's and P's) and (number of $\bar{Z}$'s and $\bar{P}$'s). The additional O(2) reflection symmetry sends $Z \leftrightarrow \bar{Z}$. With this notation, $H = \mathrm{tr}P\bar{P} + M^2\mathrm{tr}Z\bar{Z} + \frac{1}{2}\mathrm{tr}[Z, \bar{Z}]^2$ and $C = -\mathrm{i}[Z, \bar{P}] - \mathrm{i}[\bar{Z}, P] - 2$.

Because of large-N factorization, we only need to consider single-trace operators. The operators are "words" composed of "indexed letters" X_I and P_J with indices fully contracted. Since $\mathrm{Tr}X_I P_I = (D/2)\mathrm{i}N^2$, we perform the following shift [34] so that expectation values of single-trace operators are of order one in the large N limit

$$\mathrm{Tr} \to \mathrm{tr} = \frac{1}{N}\mathrm{Tr}, \quad X_I \to \frac{1}{\sqrt{N}}X_I, \quad P_I \to \frac{1}{\sqrt{N}}P_I, \quad (3)$$

For the O(2) model, we forgo the indexed notation and work with words built from the letters $\{Z, \bar{Z}, P, \bar{P}\}$. For practical implementation, it is convenient to define $\Pi \equiv -\mathrm{i}P$, so that all correlators appearing in the bootstrap are real [14].

Constraints: The dynamical constraints include the equations of motion for a stationary state

$$\langle [H, \mathcal{O}] \rangle = 0. \quad \forall\ \mathcal{O} \text{ single-trace operator.} \quad (4)$$

We refer to constraints that do not involve the explicit form of the Hamiltonian as "kinematic constraints." These include cyclicity of the trace and gauge invariance. The ground states of these models are time-reversal symmetric, which, together with Hermiticity of the matrices, implies that $\langle \mathrm{tr}\mathcal{O}_1, \ldots, \mathcal{O}_n \rangle = \pm\langle \mathrm{tr}\mathcal{O}_n, \ldots, \mathcal{O}_1 \rangle$ where we choose $+(-)$ if there are an even (odd) number of P's in the correlator [35].

We also impose positivity of the inner product

$$\mathcal{M}_{ij} = \langle \mathrm{tr}\bar{\mathcal{O}}_i \mathcal{O}_j \rangle, \qquad \mathcal{M} \succeq 0, \quad (5)$$

and ground state positivity

$$\mathcal{N}_{ij} = \langle \mathrm{tr}\bar{\mathcal{O}}_i [H, \mathcal{O}_j] \rangle, \qquad \mathcal{N} \succeq 0. \quad (6)$$

This inequality immediately follows from demanding that the state $\mathcal{O}|\Omega\rangle$ has an average energy larger than the ground state energy $E_0 = \langle\Omega|H|\Omega\rangle$. This can be viewed as the zero-temperature limit of the finite temperature bootstrap [36–39]. Note that, here, we consider adjoint operators $\mathcal{O}_i$, $\mathcal{O}_j$ with two open matrix indices. This is justified since the ground state of the ungauged model is a gauge singlet. As in [14], we decompose operators into irreps of O(D) and consider positivity for each irrep separately, as operators in different irreps are orthogonal due to group theoretical reason. For $D = 2$, this is particularly convenient, since the irreps are labeled by charge; the letters Z, P carry charge 1 and $\bar{Z}, \bar{P}$ carry charge -1. For further details, we refer the reader to Supplemental Material [33], which contains an explicit implementation of the irreducible decomposition as well as a detailed worked example of all the constraints, and also includes Refs. [40].

Hierarchy: Following the approach developed in [6,14], we introduce a hierarchy among the set of all variables, and impose bootstrap constraints up to some level of the hierarchy. The hierarchy is defined by sorting operators into levels: we assign the basic fields $\ell(X_I) = 1$, $\ell(P_I) = 2$. This assignment has the feature that

TABLE I. The number of free variables in the semidefinite programming problem (after taking the quotient by the kinematic and dynamical constraints), for the $D = 2$ and $D = 9$ models.

	$D = 2$		$D = 9$	
Level	Free variables	All variables	Free variables	All variables
4	3	14	3	7
6	8	94	10	52
8	22	614	43	487
10	77	4086	289	5737
12	326	27 830	2859	81 442
14	1569	192 374	…	1 348 057

$\ell([H, \mathcal{O}]) = \ell(\mathcal{O}) + 1$. We enumerate all variables up to a given level and taking the quotient of this space by the equality constraints. The resulting "search space" can be parametrized by a choice of "free variables" which are the actual variables that enter the semidefinite program. Table I displays the number of free variables for each level.

Nonlinear relaxation: The cyclicity of the trace relates single-trace correlators to double-trace correlators. Since we wish to work at large N, we impose large-N factorization. This implies that the single-trace correlation functions entering the matrices $\mathcal{M}$ and $\mathcal{N}$ are constrained by a set of quadratic relations. Consequently, the matrices $\mathcal{M}$ and $\mathcal{N}$ are, in general, nonlinear functions of the search-space parameters.

If the number of nonlinear parameters $\lesssim 3$, one can scan over them. However, at higher levels, the number of nonlinear parameters grows, and one should use the technique of nonlinear relaxation [4,13] [41]. The basic idea is to introduce a new variable for each double-trace that appears, e.g., $y = \langle \mathrm{tr} P_I P_I \rangle^2$. Then, we may replace the equation $y = \langle \mathrm{tr} P_J P_J \rangle^2$ with the weaker (but rigorous) inequality $y \geq (\langle \mathrm{tr} P_J P_J \rangle)^2$. This can be encoded in a positive semidefinite matrix: $\left(\begin{smallmatrix} 1 & x \\ x & y \end{smallmatrix}\right) \succeq 0$. In addition, we introduce some new positivity relations (beyond what was done in [4,13]) by imposing $y \leq \langle \mathrm{tr}(P_I P_I)(P_J P_J) \rangle$ since positivity requires $\langle \mathrm{tr}(P_I P_I)^2 \rangle \geq \langle \mathrm{tr} P_I P_I \rangle^2$. We refer the reader to Appendix B for more detailed implementation. After performing this relaxation, we are left with a standard semidefinite programming problem with an expanded set of variables [43].

Bootstrap results—We considered the bootstrap for both the massless model ($M = 0$) and the massive model with $M^2 = 1$ (equivalently, $\lambda_{\mathrm{eff}} = 1$). For the case $D = 2$, we performed a bootstrap analysis up to level 14, while for $D = 9$ the analysis was carried out up to level 11. We mainly consider the bounds for the dimensionless normalized ground state energy $\mathcal{E} \equiv (E_0/N^2)(g_{\mathrm{YM}}^2 N)^{-1/3}$ and $\langle \mathrm{tr} X^2 \rangle = (1/D)\langle \mathrm{tr} X_I X_I \rangle$ at different levels. The results are presented in Table II, Figs. 1, and 2.

For the $D = 2$ model, [44,46] we performed a Euclidean lattice computation using the Hybrid Monte Carlo algorithm. For $D = 2$, a large N and continuum extrapolation yielded the numbers that we display in Table II. For $D = 9$, one may compare to the $N = 32$ Monte Carlo lattice simulation of [11]. We also compare [47] to the interesting numerical approach of [45]. Their approach is based on a truncation of the loop equations [45,48–51].

We also bootstrapped the level 4 operator $\langle \mathrm{tr} Z^2 \bar{Z}^2 \rangle = \frac{1}{4}\sum_{I,J}\langle \mathrm{tr} X_I X_J X_I X_J \rangle$. Together with the constraints, the variables in Table II fully determine the expectation value

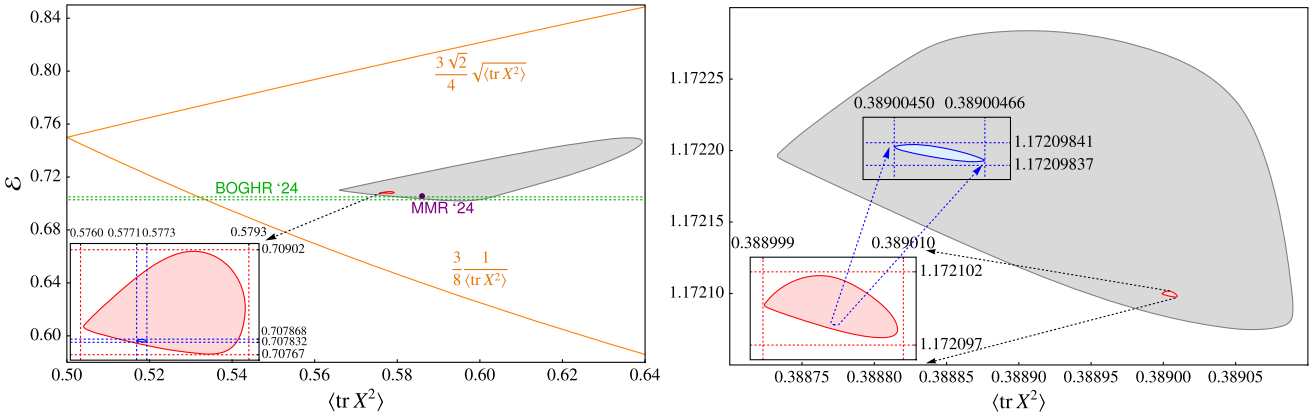


FIG. 1. Left: Bootstrap constraints on the ground state or confining phase energy $\mathcal{E} = E_0/(g_{\mathrm{YM}}^2 N)^{1/3}$ and the simplest observable $\langle \mathrm{tr} X^2 \rangle = \frac{1}{2}\langle \mathrm{tr} X_I X_I \rangle = \langle \mathrm{tr} Z\bar{Z} \rangle$ for the $D = 2$ massless matrix model. The level 6 constraint (7) for the massless $D = 2$ model has the shape of a peninsula. The feasible island first appears at level 10. The island shrinks rapidly as we go to higher levels, so we show it more clearly in the inset panel. The small level 14 island is not visible to the naked eye in the main figure. Comparison to previous numerical results in the literature [44] (green) and [45] (purple) are given. Right: the level 10, 12, and 14 constraints for the massive $D = 2$ model with $M^2 = 1$. The level 10 island already excludes the Monte Carlo result [44]. A potential future application of these tiny islands is to enable a better estimate of potential systematic uncertainties in Monte Carlo simulations.

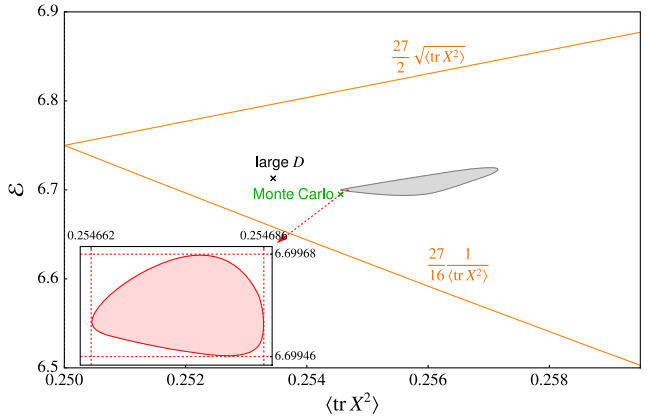


FIG. 2. Here, we display the level 10 constraints for the massless $D = 9$ model, sometimes referred to as "bosonic BFSS". The cross $\times$ indicates the estimate from the $1/D$ expansion [12] and the green $\times$ is from the $N = 32$ Monte Carlo simulation in [11], see also [20]. The orange curves are the analytic bounds (7). The level 10 island is displayed in gray; the red island (barely visible) near the western tip is the level 11 island; it is displayed more clearly in the inset panel.

of all operators up to level 4. At level 8, this operator is bounded from both sides for the massive $M^2 = 1$ model (and is unbounded from above at level 6 or below). To find a two-sided bound for the massless model, we had to go to level 10.

To build intuition for these bounds, we note that, at lower levels, it is possible to analyze the bootstrap constraints by hand and identify which inequalities are saturated. At level 5, we may derive a simple analytic bound on $\mathcal{E}$ and $\langle \mathrm{tr} X^2 \rangle$ [52]. From the concrete example presented in the Supplemental Material [33], we obtain the following bounds:

$$\frac{\mathcal{E}}{D} \geq \max\left\{\frac{3}{16\langle \mathrm{tr} X^2\rangle} + \frac{M^2\langle \mathrm{tr} X^2\rangle}{4}, M^2\langle \mathrm{tr} X^2\rangle\right\},$$
$$\frac{\mathcal{E}}{D} \leq \frac{1}{8}\left[2M^2\langle \mathrm{tr} X^2\rangle + 3[2(D-1)\langle \mathrm{tr} X^2\rangle + M^2]^{1/2}\right] \quad (7)$$

For the massless case, this yields $[1/(8D-8)^{1/3}] \leq \langle \mathrm{tr} X^2\rangle$. Surprisingly, for $M^2 = 0$, adding the bootstrap constraints up to level 8 did not lead to any improvement for these inequalities. In other words, (7) is the optimal bound up to level 8. The peninsula bound derived here is quite analogous to the level 5 peninsula in the BFSS case. The behavior of these bounds is markedly different for the massive case $M^2 > 0$. For massive models, the inequalities in (7) carve out a compact allowed region (an "island") already at level 5; the island shrinks at higher levels.

Discussion—At level $L < 10$, our results for the massless $M^2 = 0$ cases are qualitatively similar to the plots that were obtained in [14] for the maximally supersymmetric Yang-Mills matrix model (the D0-brane or BFSS matrix model). To make the comparison more concrete, note that in the supersymmetry (SUSY) case, there are three terms in the Hamiltonian $E = K + V + F$, whereas in the bosonic models, there are only two terms $E = K + V$. These terms are related by the virial theorem, $-2K + 4V + F = 0$ in the SUSY case and $-2K + 4V = 0$ in the bosonic (massless) case. However, SUSY gives an additional constraint $E = 0$ for the ground state of BFSS, so there is really only one independent variable "energy"-like variable $\mathcal{E}$ in both the SUSY and non-SUSY cases. In addition to this level 4 variable (which can be viewed as the kinetic or potential energy), there is the level 2 variable $\langle \mathrm{tr} X^2\rangle$ and one other level 4 variable $\langle \mathrm{tr} X_I X_I X_J X_J\rangle$. In all models that we studied, a peninsula in the $\langle \mathrm{tr} X^2\rangle - \mathcal{E}$ appears exactly at level 5: there is an unconditional lower bound on $\langle \mathrm{tr} X^2\rangle$ at level 5, but no upper bound. Furthermore, up to level 10,

TABLE II. Ground state energy $\mathcal{E}$ bounds and expectation values of $\langle \mathrm{tr} X_I X_I\rangle$ from bootstrap and Monte Carlo studies for various masses M^2 and dimensions D. Results in bold are level 14 bootstrap bounds; the $D = 9$ bootstrap results are level 11. Our rigorous results are complementary to the finite temperature Monte Carlo results as they do not involve any continuum or large N extrapolation.

Model	$\mathcal{E}$	$\langle \mathrm{tr} X_I X_I\rangle$	Level 4 operator
$M^2 = 0$, $D = 2$			$\langle \mathrm{tr}(Z^2\bar{Z}^2)\rangle$
Bootstrap	[**0.707 832**, **0.707 868**]	[**1.154 20**, **1.154 60**]	[**0.370 55**, **0.370 85**]
Monte Carlo [44]	0.7039(11)	…	…
Loop truncation [45]	0.7056(2)	1.172(1)	0.383(2)
Large D expansion [12]	0.756	0.985	0.177
$M^2 = 1$, $D = 2$			$\langle \mathrm{tr}(Z^2\bar{Z}^2)\rangle$
Bootstrap	[**1.172 098 376**, **1.172 098 408**]	[**0.778 008 98**, **0.778 009 34**]	[**0.158 505 88**, **0.158 506 07**]
Monte Carlo [44]	1.1654(11)	…	…
Loop truncation [45]	1.17198	0.7784	0.1588
$M^2 = 0$, $D = 9$			$\langle \mathrm{tr} X_I X_I X_J X_J\rangle$
Bootstrap	[6.699 46, 6.699 68]	[2.291 95, 2.292 18]	[5.7787, 5.7804]
Monte Carlo [11]	6.695(5)	2.291(1)	…
Large D expansion [12]	6.713	2.279	5.646

there is a "vertical" peninsula in the $\langle \mathrm{tr} X^2 \rangle - \langle \mathrm{tr} X_I X_I X_J X_J \rangle$ plot that resembles figure 3 in [14].

These features are special to the $M^2 = 0$ models. When we added a mass term, we saw that the bootstrap behaved quite differently; an island appears already at level 4. It seems that the "classically" flat directions present in these potentials make it more difficult to upper bound the size of the ground state wave function $\langle \mathrm{tr} X^2 \rangle$.

At level 10, the feasible region becomes an island in the massless $D = 2$ and $D = 9$ cases we studied in this Letter. Therefore, we are optimistic that an island will appear at level 10 (or perhaps within a few levels beyond) in the supersymmetric model. Note that, in the supersymmetric setting, ground state positivity (6) was implicitly imposed by the supercharge equations of motion [15].

An extension of our Letter to the future is to study the models at finite temperature, using the approach outlined in [38]. (One could also study observables in a microcanonical window of energies E/N^2 above the ground state.) In fact, the near agreement between our zero temperature result and the low (but $O(1)$ in 't Hooft units) temperature Monte Carlo results may already be viewed as strong evidence that these theories are in a confined phase, where simple observables are expected to be independent of temperature at leading order in $1/N^2$. Another remote but interesting possibility is that the small discrepancy between our zero temperature results and the finite temperature Monte Carlo results is not due to underestimated systematic error but, instead, represents a failure of the conjectured phase diagram. In other words, to compare our zero temperature bootstrap result with the low-temperature Monte Carlo result, we assumed that the theory is in a confined phase where to leading order in $1/N^2$ the thermal energy is independent of temperature. This assumption is supported by the Monte Carlo simulations and Eguchi-Kawai equivalence [11,44,46] but remains unproven analytically. The existence of a confined phase is expected for large D from the $1/D$ expansion [12], but, here, we can test the conjectured phase diagram even at $D = 2$.

Another interesting problem is to compute the Polyakov loop using the bootstrap formalism. This could be done by modifying the gauge constraint. Combining these two future directions, one could confirm the existence of the Gross-Wadia-Witten transition at finite D [10–12]. One could also study time-dependent correlators [39] with the eventual goal of computing the quasinormal modes [54,55].

Finally, it would be interesting to study supersymmetric models with $\mathrm{SO}(D)$ symmetry, see Refs. [46,56]. These models have fewer supersymmetries than the BFSS model; their gravity duals are much less understood compared to BFSS [57,58]. In particular, the $\mathcal{N} = 2$ SUSY model [59,60] would be an interesting bootstrap target. It would be interesting to test whether there are metastable bound states in the planar 't Hooft limit of these models, which would be akin to the D0-brane black hole in the BFSS model.

Acknowledgments—We thank Yiming Chen, Minjae Cho, Mathew Dodelson, Barak Gabai, Davide Gaiotto, Masanori Hanada, Igor Klebanov, Stephen Shenker, Jessica Yeh, and Xi Yin for discussions. We especially thank Davide Gaiotto for providing computational resources that enabled most of the results presented in this work. H. L. is supported by a Bloch Fellowship and by NSF Grant No. PHY-2310429. Z. Z. is supported by the Simons Foundation Grant No. 994308 for the Simons Collaboration on Confinement and QCD Strings.

Data availability—The data are not publicly available. The data are available from the authors upon reasonable request.

[1] P. D. Anderson and M. Kruczenski, Loop equations and bootstrap methods in the lattice, Nucl. Phys. **B921**, 702 (2017).
[2] H. W. Lin, Bootstraps to strings: Solving random matrix models with positivity, J. High Energy Phys. 06 (2020) 090.
[3] X. Han, S. A. Hartnoll, and J. Kruthoff, Bootstrapping matrix quantum mechanics, Phys. Rev. Lett. **125**, 041601 (2020).
[4] V. Kazakov and Z. Zheng, Analytic and numerical bootstrap for one-matrix model and "unsolvable" two-matrix model, J. High Energy Phys. 06 (2022) 030.
[5] Alternatively, at finite N, one may impose trace relations [6].
[6] V. Kazakov and Z. Zheng, Bootstrap for finite N lattice Yang-Mills theory, J. High Energy Phys. 03 (2025) 099.
[7] O. Aharony, J. Marsano, S. Minwalla, K. Papadodimas, and M. Van Raamsdonk, The Hagedorn—deconfinement phase transition in weakly coupled large N gauge theories, Adv. Theor. Math. Phys. **8**, 603 (2004).
[8] D. J. Gross and E. Witten, Possible third order phase transition in the large N lattice gauge theory, Phys. Rev. D **21**, 446 (1980).
[9] S. R. Wadia, $N =$ infinity phase transition in a class of exactly soluble model lattice gauge theories, Phys. Lett. **93B**, 403 (1980).
[10] O. Aharony, J. Marsano, S. Minwalla, and T. Wiseman, Black hole-black string phase transitions in thermal $1 + 1$ dimensional supersymmetric Yang-Mills theory on a circle, Classical Quantum Gravity **21**, 5169 (2004).
[11] N. Kawahara, J. Nishimura, and S. Takeuchi, Phase structure of matrix quantum mechanics at finite temperature, J. High Energy Phys. 10 (2007) 097.
[12] G. Mandal, M. Mahato, and T. Morita, Phases of one dimensional large N gauge theory in a 1/D expansion, J. High Energy Phys. 02 (2010) 034.
[13] V. Kazakov and Z. Zheng, Bootstrap for lattice Yang-Mills theory, Phys. Rev. D **107**, L051501 (2023).
[14] H. W. Lin and Z. Zheng, Bootstrapping ground state correlators in matrix theory. Part I, J. High Energy Phys. 01 (2025) 190.
[15] H. Lin and Z. Zheng, Bootstrapping BFSS, part II (to be published).

[16] D. N. Kabat, G. Lifschytz, and D. A. Lowe, Black hole thermodynamics from calculations in strongly coupled gauge theory, Int. J. Mod. Phys. A **16**, 856 (2001).
[17] K. N. Anagnostopoulos, M. Hanada, J. Nishimura, and S. Takeuchi, Monte Carlo studies of supersymmetric matrix quantum mechanics with sixteen supercharges at finite temperature, Phys. Rev. Lett. **100**, 021601 (2008).
[18] M. Hanada, Y. Hyakutake, J. Nishimura, and S. Takeuchi, Higher derivative corrections to black hole thermodynamics from supersymmetric matrix quantum mechanics, Phys. Rev. Lett. **102**, 191602 (2009).
[19] S. Catterall and T. Wiseman, Black hole thermodynamics from simulations of lattice Yang-Mills theory, Phys. Rev. D **78**, 041502 (2008).
[20] V. G. Filev and D. O'Connor, The BFSS model on the lattice, J. High Energy Phys. 05 (2016) 167.
[21] D. Kadoh and S. Kamata, Gauge/gravity duality and lattice simulations of one dimensional SYM with sixteen supercharges, arXiv:1503.08499.
[22] E. Berkowitz, E. Rinaldi, M. Hanada, G. Ishiki, S. Shimasaki, and P. Vranas, Precision lattice test of the gauge/gravity duality at large-N, Phys. Rev. D **94**, 094501 (2016).
[23] E. Berkowitz, M. Hanada, E. Rinaldi, and P. Vranas, Gauged and ungauged: A nonperturbative test, J. High Energy Phys. 06 (2018) 124.
[24] S. Pateloudis, G. Bergner, M. Hanada, E. Rinaldi, A. Schäfer, P. Vranas, H. Watanabe, and N. Bodendorfer (Monte Carlo String/M-theory (MCSMC) Collaboration), Precision test of gauge/gravity duality in D0-brane matrix model at low temperature, J. High Energy Phys. 03 (2023) 071.
[25] J. Hoppe, V. Kazakov, and I. K. Kostov, Dimensionally reduced SYM(4) as solvable matrix quantum mechanics, Nucl. Phys. **B571**, 479 (2000).
[26] B. Lucini and M. Panero, SU(N) gauge theories at large N, Phys. Rep. **526**, 93 (2013).
[27] M. Caselle, N. Magnoli, A. Nada, M. Panero, D. Panfalone, and L. Verzichelli, Confining strings in three-dimensional gauge theories beyond the Nambu-Gotō approximation, J. High Energy Phys. 08 (2024) 198.
[28] A. Athenodorou, S. Dubovsky, C. Luo, and M. Teper, Confining strings and the worldsheet axion from the lattice, Int. J. Mod. Phys. A **40**, 2540003 (2025).
[29] J. B. Kogut and L. Susskind, Hamiltonian formulation of Wilson's lattice gauge theories, Phys. Rev. D **11**, 395 (1975).
[30] See Refs. [1,6,13,31,32] for some bootstrap approaches to the Euclidean path integral approach to pure Yang-Mills theory.
[31] Z. Li and S. Zhou, Bootstrapping the Abelian lattice gauge theories, J. High Energy Phys. 08 (2024) 154.
[32] Y. Guo, Z. Li, G. Yang, and G. Zhu, Bootstrapping SU(3) lattice Yang-Mills theory, J. High Energy Phys. 12 (2025) 033.
[33] See Supplemental Material at http://link.aps.org/supplemental/10.1103/cyq8-4sd7 for additional details on the numerical implementation, the relaxation procedure, the large-D analysis, and a pedagogical example illustrating the bootstrap framework.
[34] This is equivalent to introducing a formal $\hbar = 1/N$ so that $[X_{ij}, P_{kl}] \propto \mathrm{i}\hbar$.
[35] Here O_i are single letters, e.g., an X_I or a P_J.
[36] H. Araki and G. L. Sewell, KMS conditions and local thermodynamical stability of quantum lattice systems, Commun. Math. Phys. **52**, 103 (1977).
[37] H. Fawzi, O. Fawzi, and S. O. Scalet, Certified algorithms for equilibrium states of local quantum Hamiltonians, Nat. Commun. **15**, 7394 (2024).
[38] M. Cho, B. Gabai, J. Sandor, and X. Yin, Thermal bootstrap of matrix quantum mechanics, J. High Energy Phys. 04 (2025) 186.
[39] M. Cho, B. Gabai, H. W. Lin, J. Yeh, and Z. Zheng, Bootstrapping euclidean two-point correlators, arXiv:2511.08560.
[40] P. Cvitanovic, *Group Theory: Birdtracks, Lie's, and Exceptional Groups* (Princeton University Press, Princeton, NJ, 2020).
[41] In principle, one can also consider other methods like the navigator function [42].
[42] M. Reehorst, S. Rychkov, D. Simmons-Duffin, B. Sirois, N. Su, and B. van Rees, Navigator function for the conformal bootstrap, SciPost Phys. **11**, 072 (2021).
[43] Although, in principle, we could relax all quadratic variables, we found it best to scan over $\langle \mathrm{tr} X_I X_I \rangle$ while relaxing the remaining quadratic variables.
[44] N. Bodendorfer, O. Oktay, V. Gautam, M. Hanada, and E. Rinaldi, Variational Monte Carlo with neural network quantum states for Yang-Mills matrix model, Phys. Rev. D **112**, 046010 (2025).
[45] K. Mathaba, M. Mulokwe, and J. P. Rodrigues, Large N master field optimization: the quantum mechanics of two Yang-Mills coupled matrices, J. High Energy Phys. 02 (2024) 054.
[46] E. Rinaldi, X. Han, M. Hassan, Y. Feng, F. Nori, M. McGuigan, and M. Hanada, Matrix-model simulations using quantum computing, deep learning, and lattice Monte Carlo, PRX Quantum **3**, 010324 (2022).
[47] Our $\lambda_{\mathrm{eff}} = 1$ becomes $m = 2$, $g = 2$ in the conventions of [45], after a canonical transformation.
[48] A. Jevicki, O. Karim, J. P. Rodrigues, and H. Levine, Loop space Hamiltonians and numerical methods for large N gauge theories, Nucl. Phys. **B213**, 169 (1983).
[49] A. Jevicki, O. Karim, J. P. Rodrigues, and H. Levine, Loop space Hamiltonians and numerical methods for large N gauge theories. 2., Nucl. Phys. **B230**, 299 (1984).
[50] J. P. Rodrigues, Numerical solution of lattice Schwinger-dyson equations in the large N limit, Nucl. Phys. **B260**, 350 (1985).
[51] R. d. M. Koch, A. Jevicki, X. Liu, K. Mathaba, and J. P. Rodrigues, Large N optimization for multi-matrix systems, J. High Energy Phys. 01 (2022) 168.
[52] See Refs. [53] and [14] for similar bounds in the BFSS case.
[53] H. W. Lin, Bootstrap bounds on D0-brane quantum mechanics, J. High Energy Phys. 06 (2023) 038.
[54] M. Dodelson, Ringdown in the SYK model, SciPost Phys. **19**, 081 (2025).
[55] M. Dodelson, Black holes from chaos, arXiv:2501.06170.
[56] N. Kim and J.-H. Park, Massive super Yang-Mills quantum mechanics: Classification and the relation to supermembrane, Nucl. Phys. **B759**, 249 (2006).

[57] T. Banks, W. Fischler, S. H. Shenker, and L. Susskind, M theory as a matrix model: A conjecture, Phys. Rev. D **55**, 5112 (1997).
[58] N. Itzhaki, J. M. Maldacena, J. Sonnenschein, and S. Yankielowicz, Supergravity and the large N limit of theories with sixteen supercharges, Phys. Rev. D **58**, 046004 (1998).
[59] J. Hoppe, On the construction of zero energy states in supersymmetric matrix models, arXiv:hep-th/9709132.
[60] J. Hoppe and S.-T. Yau, Absence of zero energy states in reduced SU(N) 3-d supersymmetric Yang-Mills theory, arXiv:hep-th/9711169.
[61] M. Nakata, A numerical evaluation of highly accurate multiple-precision arithmetic version of semidefinite programming solver: SDPA-GMP, -QD and -DD., in *Proceedings of the 2010 IEEE International Symposium on Computer-Aided Control System Design* (2010), pp. 29–34.
[62] F. Permenter and P. Parrilo, Partial facial reduction: Simplified, equivalent SDPS via approximations of the PSD cone, Math. Program. **171**, 1 (2017).
[63] T. Hotta, J. Nishimura, and A. Tsuchiya, Dynamical aspects of large N reduced models, Nucl. Phys. **B545**, 543 (1999).
[64] T. Anegawa, N. Iizuka, and D. Kabat, Dissipation in the 1/D expansion for planar matrix models, Phys. Rev. D **111**, 025003 (2025).
[65] J. P. Rodrigues, "Glueballs" in the quantum mechanics of three large massless Yang-Mills coupled matrices, Phys. Lett. B **868**, 139768 (2025).
[66] J. Maldacena and A. Milekhin, To gauge or not to gauge?, J. High Energy Phys. 04 (2018) 084.
[67] R. Lanzette and Z. Zheng, Upper bound on the gap of quantum system (to be published).

End Matter

Appendix A: Numerical implementation—To solve the semidefinite programming (SDP) constructed, we used SDPA-GMP, an arbitrary-precision arithmetic SDP solver [61]. We observed that our SDP problem exhibited significant numerical instability, which motivated our choice of an arbitrary-precision solver. These numerical instabilities can be traced back to the lack of strict feasibility in the primal form of the SDP. For further technical discussion of this type of numerical instability, and possible (though not systematic) strategies for mitigating it, we refer the reader to, for example, [62].

Our Github repository includes a MATHEMATICA notebook as an example for generating the final SDP. Users are free to export the output to other SDP solvers to obtain bounds on specific variables. The built-in solver in MATHEMATICA may suffice for lower bootstrap levels, but for more ambitious computations, a higher-precision solver is necessary.

Appendix B: Relaxation—In this appendix, we provide additional details on the implementation of the relaxation procedure. Let us denote by $\{\mathcal{O}_i\}$ the set of singlet operators that appear up to a given truncation level. (Here, each $\mathcal{O}_i$ must be a singlet under the global symmetry; otherwise, its expectation value vanishes.) Then, we define the corresponding column vector of expectation values,

$$x_i \equiv \langle \mathrm{tr}\mathcal{O}_i \rangle, \tag{B1}$$

so that $\vec{x}$ collects the expectation values of all singlet operators included at this level. Then, the quadratic variables are given by the elements of the following matrix Q, with entries:

$$Q_{ij} = x_i x_j, \tag{B2}$$

or, more compactly,

$$Q = \vec{x}\vec{x}^{\mathrm{T}}. \tag{B3}$$

Whenever quadratic terms appear in our constraints, we replace them with the corresponding elements of the matrix Q. In this way, we isolate the nonconvexity of our optimization problem in (B2). In the following, we study the relaxation of (B2).

We observe that the matrix Q satisfies the following two convex conditions. First, the matrix

$$\begin{pmatrix} 1 & \vec{x}^{\mathrm{T}} \\ \vec{x} & Q \end{pmatrix} \succeq 0 \tag{B4}$$

is positive semidefinite, since it is the outer product of the vector $(1, \vec{x}^{\mathrm{T}})^{\mathrm{T}}$ with itself.

Additionally, the following matrix is also positive semidefinite, as implied by (5):

$$\langle \mathrm{tr}(\mathcal{O}_i - \langle \mathcal{O}_i \rangle)^{\dagger}(\mathcal{O}_j - \langle \mathcal{O}_j \rangle) \rangle = \mathcal{M}_{ij} - Q_{ij} \succeq 0. \tag{B5}$$

In the relaxation, we introduce a new matrix $\mathcal{Q}$, which, instead of satisfying (B2), is required to satisfy the following two conditions:

$$\begin{pmatrix} 1 & \vec{x}^{\mathrm{T}} \\ \vec{x} & \mathcal{Q} \end{pmatrix} \succeq 0, \tag{B6}$$

$$\mathcal{M} \succeq \mathcal{Q}. \tag{B7}$$

Then, we replace every occurrence of an element of Q in other constraints with the corresponding element of $\mathcal{Q}$. The relaxation implementation described here, namely (B6) and (B7), is stronger than the previous approach in [4,13], where only (B6) was imposed.

Appendix C: Large D comparison—One may also compare our results in the main text with the large-D approximation of this model; see Refs. [12,63,64]. In this limit, the system can be viewed as a deformation of an $O(D)$ vector model, allowing for a controlled resummation of bubble diagrams. Details of the large-D resummation are provided in the Supplemental Material [33].

In our conventions, this gives the estimates

$$\begin{aligned}\langle \mathrm{tr} X_I X_I\rangle &= \frac{1}{2}D^{2/3}\left[1+\frac{2}{D}\left(\frac{7\sqrt{5}}{30}-\frac{9}{32}\right)+\cdots\right]\approx 2.279\\ \mathcal{E} &= D^{4/3}\left[\frac{3}{8}+\frac{1}{D}\left(\frac{\sqrt{5}}{2}-\frac{81}{64}\right)+\cdots\right]\approx 6.713\\ \langle \mathrm{tr} X_I X_I X_J X_J\rangle &= D^{4/3}\left[\frac{1}{4}+\frac{1}{D}\left(\frac{\sqrt{5}}{3}-\frac{9}{32}\right)+\cdots\right]\approx 5.646\end{aligned} \tag{C1}$$

The first two were computed in [12]; the third, to our knowledge, has not appeared in the literature and is derived in Supplemental Material [33]. According to the virial theorem, the potential energy $2V = \langle \mathrm{tr} X_I^2 X_J^2\rangle - \langle \mathrm{tr} X_I X_J X_I X_J\rangle = 2\mathcal{E}/3$. We observe that, to leading order in D, $\langle \mathrm{tr} X_I^2 X_J^2\rangle = 2\mathcal{E}/3$. This implies that the "alternating correlator" $\langle \mathrm{tr} X_I X_J X_I X_J\rangle$ at leading order in N is subleading in $1/D$ compared to $\langle \mathrm{tr} X_I^2 X_J^2\rangle$.

We have reported the numbers for $D = 9$ in (C1). Although it is a bit extreme, one can also try $D = 2$; one obtains estimates which are unsurprisingly less accurate than for $D = 9$. It would be interesting to repeat the bootstrap at various values of D to better test the large D scaling. Some results for $D = 3$ using the loop truncation method have already been obtained [65].

Appendix D: The adjoint sector—Let us comment on gauge nonsinglet states in matrix quantum mechanics. A basic quantity is the energy gap to the adjoint sector ΔE_{adj}. This quantity is related to the adjoint Polyakov loop at low temperatures $P \sim e^{-\beta \Delta E_{\mathrm{adj}}}$. Here, we present a simple bootstrap bound

$$\Delta\mathcal{E}_{\mathrm{adj}} = \Delta E_{\mathrm{adj}}(g_{\mathrm{YM}}^2 N)^{-1/3} \le \frac{\langle \mathrm{tr} X_I [H, X_I]\rangle}{\langle \mathrm{tr} X_I X_I\rangle} = \frac{1}{2\langle \mathrm{tr} X^2\rangle} \tag{D1}$$

where we have used the ground state positivity matrix (6). (We also give a different derivation of this bound in [39], by bootstrapping time-dependent correlators.)

Combined with our level 11 lower bound on $\langle \mathrm{tr} X^2\rangle$, we have the following comparison with the Monte Carlo estimate [23]:

$$\Delta\mathcal{E}_{\mathrm{adj}} \le 1.963\,39, \qquad \Delta\mathcal{E}_{\mathrm{adj}}^{\mathrm{Monte\ Carlo}} \approx 2.043(76). \tag{D2}$$

This estimate applies to the $D = 9$, $M = 0$ model. The Monte Carlo estimate [23] was obtained by contrasting the gauged and ungauged thermodynamics; Reference [23] also reports an alternative estimate based on measuring $\langle \mathrm{tr} X^2\rangle$ in the ungauged model, yielding

$$\Delta\mathcal{E}_{\mathrm{adj}}^{\mathrm{Monte\ Carlo}} \lesssim 1.936(71).$$

At first sight, it may seem surprising that the relatively simple bound (D1) essentially reproduces the Monte Carlo value. The reason is that the bound (D1) becomes saturated in the large-D limit. At infinite D, the state $X_{ij}|\Omega\rangle$ is an energy eigenstate; this follows from the expressions for the propagator in Supplemental Material [33], which takes the form of a massive harmonic oscillator.

In the supersymmetric BFSS model [23,66], our rigorous lower bounds imply

$$\Delta\mathcal{E}_{\mathrm{adj}} \le 1.41(g_{\mathrm{YM}}^2 N)^{1/3}.$$

If we incorporate the Monte Carlo result for $\langle \mathrm{tr} X^2\rangle \approx 0.378$ [24], which lies slightly above our level-9 lower bound [14], the estimate improves to

$$\Delta\mathcal{E}_{\mathrm{adj}} \lesssim 1.3.$$

Meanwhile, the dedicated Monte Carlo study [23] finds

$$\Delta\mathcal{E}_{\mathrm{adj}} \approx 0.92(11)(g_{\mathrm{YM}}^2 N)^{1/3}.$$

Taken together, the Monte Carlo results [23,24] indicate that—unlike the bosonic $D = 9$ model—the supersymmetric theory does not come close to saturating the general bound (D1). This reflects the genuinely nontrivial dynamics governing the low-energy limit of the supersymmetric BFSS model.

In fact, the simple bound (D1) can be improved by simply considering operators other than X_I. For example, one can consider both X_I and P_I and use the full ground state positivity matrix (6); this leads to an improved bound

$$\Delta\mathcal{E}_{\mathrm{adj}} \le -\frac{1}{4px-1}\times\left(\sqrt{[p-2(D-1)x^2]^2-(4px-1)[2(D-1)x-4p^2]}-2(D-1)x^2+p\right). \tag{D3}$$

with $p = \langle \mathrm{tr} P_I P_I\rangle/D, x = \langle \mathrm{tr} X_I X_I\rangle/D$. A method to systematically bound the gap will be reported in upcoming work [67], we hope to apply this method to BFSS in the future [15].